Coexisting hidden attractors in a 4D segmented disc dynamo with one stable equilibrium or a line equilibrium*

Jianghong Bao(鲍江宏)† and Dandan Chen(陈丹丹)

School of Mathematics, South China University of Technology, Guangzhou 510641, *China*

(Received 23 February 2017; revised manuscript received 16 April 2017; published online 10 July 2017)

This paper introduces a four-dimensional (4D) segmented disc dynamo which possesses coexisting hidden attractors with one stable equilibrium or a line equilibrium when parameters vary. In addition, by choosing an appropriate bifurcation parameter, the paper proves that Hopf bifurcation and pitchfork bifurcation occur in the system. The ultimate bound is also estimated. Some numerical investigations are also exploited to demonstrate and visualize the corresponding theoretical results.

Keywords: coexisting hidden attractors, 4D segmented disc dynamo, pitchfork bifurcation, Hopf bifurcation, ultimate bound estimation

PACS: 02.30.Hq, 02.30.Oz, 05.45.–a **DOI:** 10.1088/1674-1056/26/8/080201

1. Introduction

In the last few decades, chaos, bifurcation and stability in dynamic systems have been extensively studied, since they are the main sources leading to hidden attractors, hyperchaos or other poor performance of a system.[1–5]

Hidden attractors represent a new interesting topic and attract considerable attention. They are important in engineering applications because they allow unexpected and potentially disastrous responses to perturbations in a structure like a bridge or an airplane wing.[6] They exist in systems with a stable equilibrium,[7–9] a line equilibrium[10] or no equilibria.[5,6] Wei studied hidden hyperchaotic attractors with no equilibria[6] and with only one stable equilibrium.[7] Jafari and Sprott studied chaotic attractors of three-dimensional (3D) systems with a line equilibrium.[10]

Theoretically analyzing local and global characteristics is essential for understanding of what is meant by chaos and hyperchaos, such as pitchfork bifurcation, Hopf bifurcation, ultimate bound and some other complex dynamical behaviors, which also show that these systems have rich nonlinear dynamics and are of significance in practical application.[11]

Four or higher dimensional chaotic and hyperchaotic dynamical systems modeling a natural phenomenon have been discovered to present nature more explicitly than the 3D systems.[5] Identifying and locating coexisting attractors are also crucial for studying the behavior of nonlinear systems, which become more difficult for hidden or rare states. Based on the segmented disc dynamo,[12] we introduce a 4D self-exciting segmented disc dynamo with hidden hyperchaotic attractors. The research on the novel system will feed into more studies of high dimensional systems, and also help to identify the geometrical characteristics of lower dimensional chaotic attractors. We hope that the work will shed light on more systematic studies of the segmented disc dynamo.

The proposed 4D self-exciting segmented disc dynamo possesses coexisting hidden attractors with only one stable equilibrium or a line equilibrium when parameters vary. As far as we know, it is new. It also satisfies two of the criteria introduced by Sprott:[13] (i) The system should credibly model some important unsolved problems in nature and shed insight on that problem; (ii) The system should exhibit some behavior previously unobserved.

Then by using the center manifold theorem and bifurcation theory,[14,15] we analyze the Hopf bifurcation and pitchfork bifurcation of the novel system. The ultimate bound of the system is estimated by combining the unified approach and the optimization idea.[16] Numerical investigations are also used to demonstrate the corresponding theoretical results for the two bifurcations and the ultimate boundary region.

The paper is organized as follows. We introduce a new system with only one stable equilibrium or a line equilibrium in Section 2. The Hopf bifurcation is investigated in Section 3 and in Section 4 we analyze the pitchfork bifurcation. Section 5 studies the ultimate bound. Finally, we conclude the paper in Section 6.

2. A 4D Segmented Disc Dynamo

The segmented disc dynamo is introduced by Moffatt as follows:[12]

$$\begin{cases} \dot{x}(t) = r(y-x), \\ \dot{y}(t) = mx-(1+m)y+xz, \\ \dot{z}(t) = g(mx^2+1-(1+m)xy). \end{cases}$$

*Project supported by the National Natural Science Foundation of China (Grant No. 11671149).

†Corresponding author. E-mail: majhbao@yahoo.com

© 2017 Chinese Physical Society and IOP Publishing Ltd

Based on the above system, we propose a 4D segmented disc dynamo

$$\begin{cases} \dot{x}(t) = r(y-x), \\ \dot{y}(t) = mx-(1+m)y+xz+w, \\ \dot{z}(t) = g(mx^2+1-(1+m)xy)-k_1-k_3z, \\ \dot{w}(t) = -k_2x+xz-w, \end{cases} \tag{1}$$

where $r>0,\ m>0,\ k_3\geq 0$.

System (1) is invariant under the transformation:

$$(x,y,z,w)\rightarrow(-x,-y,z,-w).$$

Namely, it has rotation symmetry around the z axis. The divergence of the system is $\nabla\cdot V=-r-m-k_3-2$, and it is dissipative. Figure 1 shows the spectrum of Lyapunov exponents and the corresponding bifurcation diagram versus $k_2\in[-3,1]$.

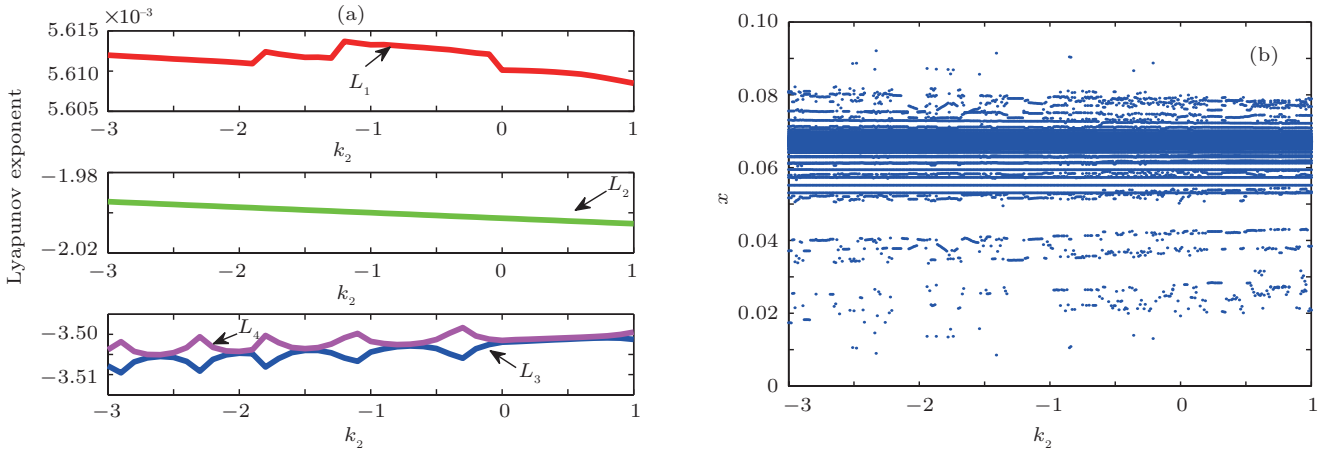


Fig. 1. (color online) Parameters $(m,r,g,k_1,k_3)=(1,\ 6,\ 12,\ 12,\ 0)$ and $k_2\in[-3,1]$, initial condition (10, 200, 30 230); (a) Lyapunov exponents spectrum of system (1); (b) Bifurcation diagram of system (1).

2.1. Equilibria and stability

For $k_1=g$ and $k_3=0$, system (1) only has a line equilibrium $(0,0,z,0)$. For $g(2(g-k_1)-(k_2+1)k_3)<0$ and $k_3\neq 0$, system (1) only has one equilibrium $P_0[0,\ 0,\ (g-k_1)/k_3,\ 0]$. The corresponding characteristic equation at P_0 is of the following form

$$(\lambda+k_3)\left(\lambda^3+(m+r+2)\lambda^2+\left((m+2r+1)+\frac{r(k_1-g)}{k_3}\right)\lambda+r\left((k_2+1)+\frac{2(k_1-g)}{k_3}\right)\right)=0. \tag{2}$$

According to the Routh–Hurwitz criterion, the real parts of all the roots λ are negative if and only if

$$\Delta_1=m+r+2>0,$$

$$\Delta_2=\begin{vmatrix} m+r+2 & r\left((k_2+1)+\dfrac{2(k_1-g)}{k_3}\right) \\ 1 & (m+2r+1)+\dfrac{r(k_1-g)}{k_3} \end{vmatrix}=\frac{(m+r+2)(k_3(m+2r+1)-(g-k_1)r)}{k_3}>0,$$

$$\Delta_3=\begin{vmatrix} m+r+2 & r\left((k_2+1)+\dfrac{2(k_1-g)}{k_3}\right) & 0 \\ 1 & (m+2r+1)+\dfrac{r(k_1-g)}{k_3} & 0 \\ 0 & m+r+2 & r\left((k_2+1)+\dfrac{2(k_1-g)}{k_3}\right) \end{vmatrix}$$

$$=\frac{r(2(g-k_1)-(k_2+1)k_3)\left(r^2(g-k_1-2k_3)+r((g-k_1)m+k_3(k_2-3m-4))-k_3(m+2)(m+1)\right)}{k_3^2}>0.$$

From these inequalities, there are

$$k_3(m+2r+1)-(g-k_1)r>0,$$

$$(2(g-k_1)-(k_2+1)k_3)\left(r^2(g-k_1-2k_3)+r((g-k_1)m+k_3(k_2-3m-4))-k_3(m+2)(m+1)\right)>0.$$

When $k_1 = g$, the above inequalities are simplified as the following form

$$(k_2+1)\left(2r^2+(3m+4-k_2)r+(m+2)(m+1)\right)>0. \quad (3)$$

The equilibrium P_0 is asymptotically stable with condition (3).

2.2. Coexistence of hidden hyperchaotic and chaotic attractors with only one stable equilibrium

When

$$(m,r,g,k_1,k_2,k_3) = (0.01,\ 0.021,\ 12,\ 12,\ 100,\ 0.001),$$

equation (1) only has one stable equilibrium $O(0,0,0,0)$ and the eigenvalues at $O(0,0,0,0)$ are

$$-0.001, -2.0280, -0.0015 \pm 1.0227\mathrm{i}.$$

(i) For initial condition $(0.5268, 7.3786, 2.6912, 4.2284)$, the Lyapunov exponents of the system (1) are $L_1 = 0.0182$, $L_2 = 0.0023$, $L_3 = -0.0228$, $L_4 = -2.0297$, and the fractional dimension is 2.8991. A hyperchaotic attractor with a stable equilibrium $(0,0,0,0)$ can be obtained (see Fig. 2(a)). Figure 2(b) shows the Poincare map.

(ii) For initial condition $(0, 7.3786, 2.6912, 4.2284)$, the trajectories of the system (1) converge on a chaotic attractor. The Lyapunov exponents of the system are $L_1 = 0.0172$, $L_2 = -0.0076$, $L_3 = -0.0074$, $L_4 = -2.0342$ and the fractional dimension is 3.0011.

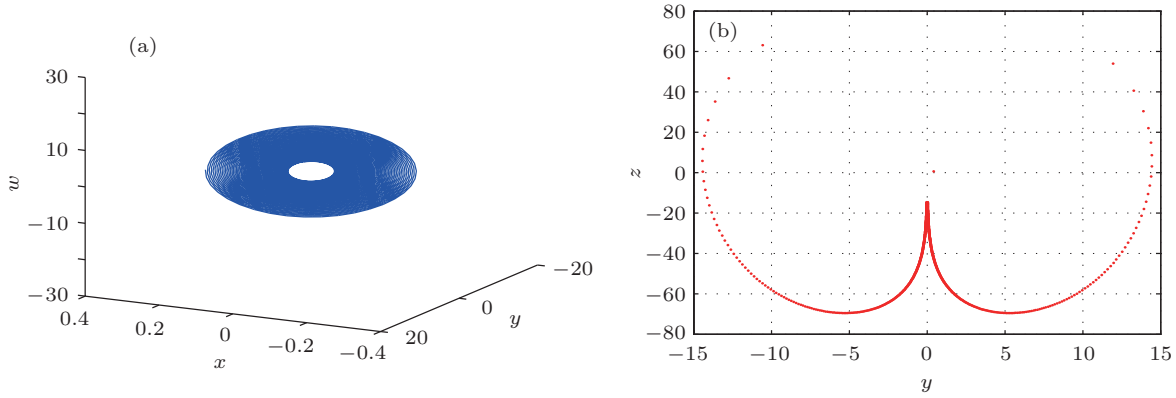


Fig. 2. (color online) Parameters $(m,r,g,k_1,k_2,k_3) = (0.01,\ 0.021,\ 12,\ 12,\ 100,\ 0.001)$, initial condition $(0.5268, 7.3786, 2.6912, 4.2284)$; (a) hyperchaotic attractor of system (1); (b) Poincaré map on the y–z plane.

2.3. Coexistence of hidden hyperchaotic and chaotic attractors with a line equilibrium

When $(m,r,g,k_1,k_2,k_3) = (1,\ 6,\ 12,\ 12,\ 100,\ 0)$, the system (1) only has a line equilibrium $(0,0,z,0)$.

i) For initial condition $(0,0,0,0)$, the Lyapunov exponents of the system (1) are found to be $L_1 = 1.5132$, $L_2 = 1.5160$, $L_3 = 0.0000$, $L_4 = -12.0292$ and the fractional dimension is 3.2518. A hyperchaotic attractor can be obtained.

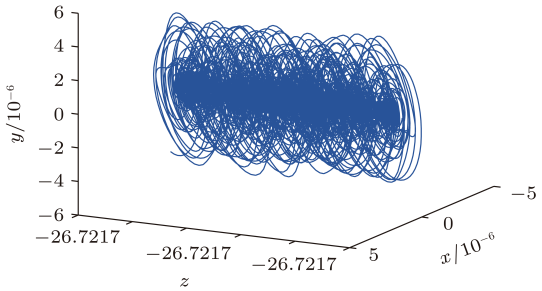


Fig. 3. (color online) Chaotic attractor of the system (1) with initial condition $(3,0,0,0)$ for $(m,r,g,k_1,k_2,k_3) = (1,6,12,12,100,0)$.

ii) For initial condition $(3,0,0,0)$, the Lyapunov exponents of the system are

$$L_1 = 0.0022, \quad L_2 = -1.5649,$$
$$L_3 = -1.5720, \quad L_4 = -5.8653$$

and the fractional dimension is 1.0014. The trajectories of the system (1) converge on a chaotic attractor (as shown in Fig. 3).

3. Hopf bifurcations in system (1)

The section utilizes the projection method described in Ref. [14] to calculate the first Lyapunov coefficient associated with the Hopf bifurcation.

For $k_3 \neq 0$, the system (1) has an equilibrium $P_0[0,\ 0,\ (g-k_1)/k_3,\ 0]$. The corresponding characteristic equation at P_0 is Eq. (2).

Let

$$f(\lambda) = \lambda^3 + (m+r+2)\lambda^2 + \left((m+2r+1) + \frac{r(k_1-g)}{k_3}\right)\lambda + r\left((k_2+1) + \frac{2(k_1-g)}{k_3}\right),$$

$$\omega = \frac{\sqrt{k_3}\sqrt{(k_1-g)r + k_3(m+2r+1)}}{k_3},$$

$$k_2^0 = \frac{k_3(m+2r+2)(m+r+1) - r(m+r)(g-k_1)}{k_3 r},$$

$$S=\left\{(m,r,g,k_1,k_2,k_3)\,|m>0,r>0,k_3\geq 0,(k_1-g)\,r+k_3\,(m+2r+1)>0,k_2=k_2^0\right\}.$$

When $(m,r,g,k_1,k_2,k_3)\in S$, the system (1) possesses two negative real roots $-m-r-2,-k_3$ and conjugate purely imaginary roots $\pm\omega\mathrm{i}$ at $P_0\,[0,0,(g-k_1)/k_3,0]$.

Substituting $\lambda=\alpha\,(k_2)+\mathrm{i}\,\omega\,(k_2)$ into $f(\lambda)=0$ and differentiating $f(\lambda)=0$ with respect to k_2 give

$$\frac{\mathrm{d}\lambda\,(k_2)}{\mathrm{d}k_2}=-\frac{k_3 r}{3k_3\lambda^2+2k_3(m+r+2)\lambda+(r\,(k_1-g)+k_3\,(m+2r+1))}.$$

Considering that $\pm\omega\mathrm{i}$ are the roots of $f(\lambda)=0$, we have

$$\frac{\mathrm{d}\lambda\,(k_2)}{\mathrm{d}k_2}\Big|_{k_2=k_2^0}=\frac{k_3 r}{3k_3\omega^2-2k_3(m+r+2)\omega\mathrm{i}-((k_1-g)\,r+k_3\,(m+2r+1))}.$$

Hence the transversality condition

$$\mathrm{Re}\left(\lambda'\,(k)\right)\Big|_{k=k_2^0}=\frac{r}{2(m+r+2)^2+2\omega^2}>0 \tag{4}$$

is also satisfied, and Hopf bifurcation at P_0 occurs. The stability of the transversal Hopf point depends on the value of the first Lyapunov coefficient, as stated in the following theorem.

Theorem 1 Considering the system (1), the first Lyapunov coefficient at $P_0\,[0,\,0,\,(g-k_1)/k_3,\,0]$ for parameter values $(m,r,g,k_1,k_2,k_3)\in S$ is given by

$$l_1=-\frac{gr^2\left(2\omega^4\,(k_3\,(m+1)+4r)+\omega^2\left(3{k_3}^2\,(m+r+1)-2k_3\,(2m+3r+2)-16r\right)-6{k_3}^2 r\right)}{k_3(m+r+1)^3\left({k_3}^2+4\omega^2\right)(\omega^2+1)^2\omega}.$$

(I) If $l_1>0$, the system (1) has a transversal Hopf point at P_0 and the Hopf point is unstable (weak repelling focus). Moreover, for each $k_2<k_2^0$, but close to k_2^0, there exists an unstable limit cycle near the stable equilibrium P_0.

(II) If $l_1<0$, the system (1) has a transversal Hopf point at P_0 and the Hopf point is stable (weak attractor focus). Moreover, for each $k_2>k_2^0$, but close to k_2^0, there exists a stable limit cycle near the unstable equilibrium P_0.

Proof By the changes

$$\begin{cases}x=x,\\ y=y,\\ z_1=z-\dfrac{g-k_1}{k_3},\\ w=w,\end{cases}$$

the system (1) becomes the following system (still denoted by x,y,z,w)

$$\begin{cases}\dot{x}(t)=r\,(y-x),\\ \dot{y}(t)=\left(m+\dfrac{g-k_1}{k_3}\right)x-(1+m)\,y+xz+w,\\ \dot{z}(t)=gmx^2-g\,(1+m)\,xy-k_3 z,\\ \dot{w}(t)=\dfrac{g-k_2k_3-k_1}{k_3}x+xz-w,\end{cases}$$

and the equilibrium P_0 is moved to $O\,[0,0,0,0]$.

From Eq. (4), the transversality condition holds. Now, we calculate the Lyapunov coefficient, which shows the stability of the equilibrium and the periodic orbit which appears.

According to Ref. [14], for the parameters $(m,r,g,k_1,k_2,k_3)\in S$, we have $\lambda_1=-m-r-2,\lambda_2=-k_3,\lambda_{3,4}=\pm\omega\mathrm{i}$, and

$$A=\begin{pmatrix}-r & r & 0 & 0\\ m+\dfrac{g-k_1}{k_3} & -1-m & 0 & 1\\ 0 & 0 & -k_3 & 0\\ -\dfrac{(m+r+1)(\omega^2+1)}{r} & 0 & 0 & -1\end{pmatrix},$$

$$p=\begin{pmatrix}-\dfrac{\mathrm{i}(\omega\mathrm{i}-m-1)(m+r+1)(\omega^2+1)}{2(\omega\mathrm{i}-r-m-2)\omega r}\\ \dfrac{\mathrm{i}(m+r+1)(\omega^2+1)}{2(\omega\mathrm{i}-r-m-2)\omega}\\ 0\\ \dfrac{(m+r+1)(\mathrm{i}-\omega)}{2(\omega\mathrm{i}-r-m-2)\omega}\end{pmatrix},$$

$$q=\begin{pmatrix}-\dfrac{r\mathrm{i}}{(m+r+1)\,(\omega+\mathrm{i})}\\ \dfrac{\omega-r\mathrm{i}}{(m+r+1)\,(\omega+\mathrm{i})}\\ 0\\ 1\end{pmatrix},$$

$$B(x,y)=\begin{pmatrix}0\\ x_1y_3+x_3y_1\\ 2gmx_1y_1-g\,(1+m)\,(x_1y_2+x_2y_1)\\ x_1y_3+x_3y_1\end{pmatrix},$$

$$C(x,y,z)=\begin{pmatrix}0\\ 0\\ 0\\ 0\end{pmatrix}.$$

Then we can compute the following values:

$$A^{-1}B(q,\bar{q}) = \begin{pmatrix} 0 \\ 0 \\ \dfrac{2r^2 g}{(m+r+1)^2(\omega^2+1)k_3} \\ 0 \end{pmatrix},$$

$$(2\omega iE - A)^{-1}B(q,q) = \begin{pmatrix} 0 \\ 0 \\ \dfrac{2r^2 g}{(m+r+1)^2(\omega^2+1)k_3} \\ 0 \end{pmatrix}.$$

Therefore

$$\begin{aligned} l_1 &= \frac{1}{2\omega}\mathrm{Re}\left[\langle p, C(q,q,\bar{q})\rangle - 2\langle p, B\left(q, A^{-1}B(q,\bar{q})\right)\rangle + \left\langle p, B\left(\bar{q}, (2\omega \mathrm{i}E - A)^{-1}B(q,q)\right)\right\rangle\right] \\ &= -\frac{gr^2\left(2\omega^4(k_3 m + k_3 + 4r) + \omega^2\left(3k_3^2(m+r+1) - 2k_3(2m+3r+2) - 16r\right) - 6rk_3^2\right)}{k_3\omega\left(k_3^2+4\omega^2\right)(m+r+1)^3(\omega^2+1)^2}. \end{aligned}$$

We preformed the numerical simulations and the results are presented below. For

$$(m, r, g, k_1, k_3) = (0.1, 1.3, -11.2, 12, 0.1),$$

one has $l_1 = 0.0067$. An unstable limit cycle with the initial condition $(0.0656, 0.0036, -231.9151, 0.09340)$ is obtained for $k_2 = 333.3769$ (See Fig. 4).

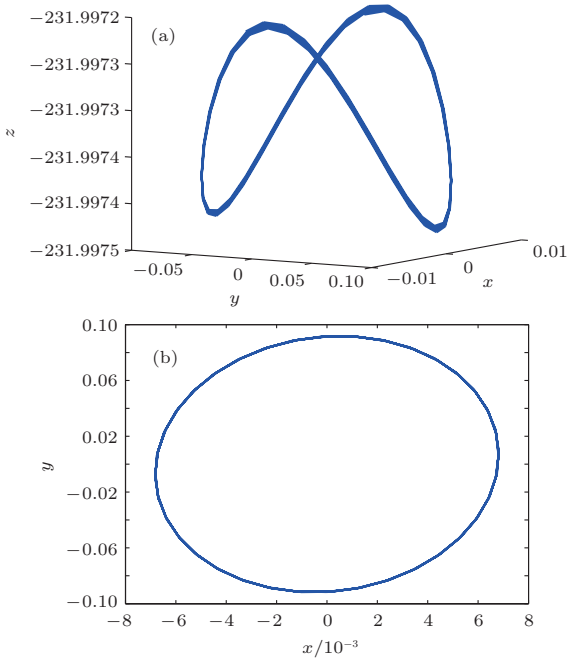


Fig. 4. (color online) A unstable limit cycle of the system (1) with initial condition $(0.0656, 0.0036, -231.9151, 0.09340)$ for $(m, r, g, k_1, k_2, k_3) = (0.1, 1.3, -11.2, 12, 333.3769, 0.1)$.

4. Pitchfork bifurcations in system (1)

We employ the center manifold theorem[15] to study the pitchfork bifurcation of the system (1).

Let

$$S = \left\{(m, r, g, k_1, k_2, k_3) \,\middle|\, r > 0, m > 0, g > 0, k_3 > 0, k_1 = g, k_2 = -1\right\}.$$

For $(m, r, g, k_1, k_2, k_3) \in S$, the system (1) only has an equilibrium $O[0,0,0,0]$. By Eq. (2), the eigenvalues at O are

$$\lambda_1 = 0, \quad \lambda_2 = -k_3,$$

$$\lambda_{3,4} = -\frac{1}{2}(m+r+2) \pm \frac{1}{2}\sqrt{(m+r)^2 - 4r}.$$

$O[0,0,0,0]$ is nonhyperbolic, and then we can obtain the following theorem.

Theorem 2 For $(m, r, g, k_1, k_2, k_3) \in S$, the system (1) undergoes a pitchfork bifurcation at $O[0,0,0,0]$. Moreover, when $k_2 > -1$, there is only one equilibrium O which is stable near the right-hand side of $k_2 = -1$; when $k_2 < -1$, O becomes unstable and the other two equilibria are stable near the left-hand side of $k_2 = -1$.

Proof The corresponding eigenvectors are

$$v_1 = \begin{pmatrix} 1 \\ 1 \\ 0 \\ 1 \end{pmatrix}, \quad v_2 = \begin{pmatrix} 0 \\ 0 \\ 1 \\ 0 \end{pmatrix},$$

$$v_3 = \begin{pmatrix} \dfrac{r(1-m(r-1))}{((m+1)\lambda_3 + m(m+r+2)+1)(\lambda_3+r)} \\ \dfrac{1-m(r-1)}{(m+1)\lambda_3 + m(m+r+2)+1} \\ 0 \\ 1 \end{pmatrix},$$

$$v_4 = \begin{pmatrix} \dfrac{r(1-m(r-1))}{((m+1)\lambda_4 + m(m+r+2)+1)(\lambda_4+r)} \\ \dfrac{1-m(r-1)}{(m+1)\lambda_4 + m(m+r+2)+1} \\ 0 \\ 1 \end{pmatrix}.$$

Let

$$k_2 = -1 + \varepsilon, \quad T = (v_1, v_2, v_3, v_4),$$
$$(x, y, z, w)^{\mathrm{T}} = T(x_1, y_1, z_1, w_1)^{\mathrm{T}}. \tag{5}$$

By Eq. (5), the system (1) becomes

$$\begin{cases} \begin{pmatrix} \dot{x}_1 \\ \dot{y}_1 \\ \dot{z}_1 \\ \dot{w}_1 \end{pmatrix} = \begin{pmatrix} 0 & 0 & 0 & 0 \\ 0 & -k_3 & 0 & 0 \\ 0 & 0 & \lambda_3 & 0 \\ 0 & 0 & 0 & \lambda_4 \end{pmatrix} \begin{pmatrix} x_1 \\ y_1 \\ z_1 \\ w_1 \end{pmatrix} + \begin{pmatrix} g_1 \\ g_2 \\ g_3 \\ g_4 \end{pmatrix}, \\ \dot{\varepsilon} = 0, \end{cases} \tag{6}$$

where

$$
\begin{aligned}
a &= \frac{(mr-m-1)z_1}{((m+1)\lambda_3+m(m+r+2)+1)(\lambda_3+r)},\\
b &= \frac{(mr-m-1)w_1}{((m+1)\lambda_4+m(m+r+2)+1)(\lambda_4+r)},\\
g_1 &= \frac{r}{2r+m+1}(x_1-ra-rb)(2y_1-\varepsilon),\\
g_2 &= g(ra+rb-x_1)(x_1-((m+1)\lambda_3+r)a-((m+1)\lambda_4+r)b),\\
g_3 &= \frac{ra+rb-x_1}{(\lambda_3-\lambda_4)(2r+m+1)}\left(\frac{\lambda_4\varepsilon(\lambda_3+r)((m+1)\lambda_3+m(m+r+2)+1)}{m+1-mr}+ry_1\right),\\
g_4 &= \frac{x_1-ra-rb}{(\lambda_3-\lambda_4)(2r+m+1)}\left(\frac{\lambda_3\varepsilon(\lambda_4+r)((m+1)\lambda_4+m(m+r+2)+1)}{m+1-mr}+ry_1\right).
\end{aligned}
$$

Thus, from the center manifold theory, a center manifold exists for Eq. (6), which can be represented locally as a graph over the variables x_1 and ε as follows:

$$
\begin{aligned}
W_c(0) = \{&(x_1,y_1,z_1,w_1,\varepsilon)\in R^4 \,|\, y_1=h_1(x_1,\varepsilon), z_1=h_2(x_1,\varepsilon), w_1=h_3(x_1,\varepsilon), |x_1|<\delta, |\varepsilon|<\bar{\delta},\\
&h_i(0,0)=0, Dh_i(0,0)=0,\ i=1,2,3\},
\end{aligned}
$$

where δ and $\bar{\delta}$ are sufficiently small.

Assume that

$$
\begin{cases}
y_1 = h_1(x_1,\varepsilon) = a_1{x_1}^2 + a_2x_1\varepsilon + a_3\varepsilon^2 + o(3),\\
z_1 = h_2(x_1,\varepsilon) = b_1{x_1}^2 + b_2x_1\varepsilon + b_3\varepsilon^2 + o(3),\\
w_1 = h_3(x_1,\varepsilon) = c_1{x_1}^2 + c_2x_1\varepsilon + c_3\varepsilon^2 + o(3).
\end{cases} \tag{7}
$$

Considering $\dot{\varepsilon}\equiv 0$, the center manifold must satisfy

$$
N(h(x_1,\varepsilon)) \triangleq D_{x_1}h\cdot g_1 - Bh - g \equiv 0, \tag{8}
$$

where

$$
h(x_1,\varepsilon) = \begin{pmatrix} h_1\\ h_2\\ h_3\end{pmatrix},\ D_{x_1}h = \begin{pmatrix} \partial h_1/\partial x_1\\ \partial h_2/\partial x_1\\ \partial h_3/\partial x_1\end{pmatrix},
$$

$$
g = \begin{pmatrix} g_2\\ g_3\\ g_4\end{pmatrix},\ B = \begin{pmatrix} -k_3 & 0 & 0\\ 0 & \lambda_3 & 0\\ 0 & 0 & \lambda_4\end{pmatrix}.
$$

Substituting Eq. (7) into Eq. (8) gives

$$
\begin{cases}
a_1 = -\dfrac{g}{k_3},\ a_2=0,\ a_3=0,\\
b_1=0,\ b_2 = \dfrac{\lambda_4(\lambda_3+r)((m+1)\lambda_3+m(m+r+2)+1)}{\lambda_3(\lambda_3-\lambda_4)(m+1-mr)(2r+m+1)},\ b_3=0,\\
c_1=0,\ c_2 = -\dfrac{\lambda_3(\lambda_4+r)((m+1)\lambda_4+m(m+r+2)+1)}{\lambda_4(\lambda_3-\lambda_4)(m+1-mr)(2r+m+1)},\ c_3=0,
\end{cases}
$$

and we obtain

$$
\begin{cases}
y_1 = h_1(x_1,\varepsilon) = -\dfrac{g}{k_3}{x_1}^2 + o(3),\\
z_1 = h_2(x_1,\varepsilon) = \dfrac{\lambda_4(\lambda_3+r)((m+1)\lambda_3+m(m+r+2)+1)}{\lambda_3(\lambda_3-\lambda_4)(\lambda_3\lambda_4(m+1)-mr(2r+m+1))}x_1\varepsilon + o(3),\\
w_1 = h_3(x_1,\varepsilon) = -\dfrac{\lambda_3(\lambda_4+r)((m+1)\lambda_4+m(m+r+2)+1)}{\lambda_4(\lambda_3-\lambda_4)(\lambda_3\lambda_4(m+1)-mr(2r+m+1))}x_1\varepsilon + o(3).
\end{cases} \tag{9}
$$

By substituting Eqs. (9) into $\dot{x}_1 = g_1$ of Eq. (6) and reducing the vector field to the center manifold, we obtain the following expressions

$$
\begin{cases}
\dot{x}_1 = F(x_1,\varepsilon) + o(4),\\
\dot{\varepsilon} = 0,
\end{cases} \tag{10}
$$

where

$$
\begin{aligned}
F(x_1,\varepsilon) = &-\frac{r\varepsilon}{2r+m+1}\left(1+\frac{r(m+r+2)}{(2r+m+1)^2}\varepsilon\right)x_1\\
&-\frac{2gr}{k_3(2r+m+1))}{x_1}^3.
\end{aligned} \tag{11}
$$

$F(x_1,\varepsilon)$ satisfies the following conditions:

$$\begin{cases} F(0,0)=0, \ \left.\dfrac{\partial F}{\partial x_1}\right|_{(0,0)}=0, \ \left.\dfrac{\partial F}{\partial \varepsilon}\right|_{(0,0)}=0, \\ \left.\dfrac{\partial^2 F}{\partial x_1^2}\right|_{(0,0)}=0, \ \left.\dfrac{\partial^2 F}{\partial x_1 \partial \varepsilon}\right|_{(0,0)}=-\dfrac{r}{2r+m+1}\neq 0, \\ \left.\dfrac{\partial^3 F}{\partial x_1^3}\right|_{(0,0)}=-\dfrac{12gr}{k_3(2r+m+1)}\neq 0. \end{cases}$$

Hence the equilibrium $(x_1,\varepsilon)=(0,0)$ of Eqs. (10) undergoes a pitchfork bifurcation at $\varepsilon=0\,(k_2=-1)$. Since

$$-\frac{\partial^3 F}{\partial {x_1}^3}\Big/\frac{\partial^2 F}{\partial x_1 \partial \varepsilon}<0,$$

the bifurcation direction is near the left-hand side $\varepsilon=0\,(k_2=-1)$. So Theorem 2 is proved.

According to Ref. [15], the restriction of the system to the center manifold is locally topologically equivalent near the bifurcating equilibrium point to the normal form, which reduces the dimensionality of the system and eliminates the nonlinearity. Hence the flow of the system (1) restricted to the center manifold of the origin, associated with the zero eigenvalue, is governed by Eq. (10). Since the invariant center manifold exists in a sufficiently small neighborhood in both x and ε of $(x,\varepsilon)=(0,0)$, all bifurcating solutions will be contained in the lower dimensional center manifold.

A more complex pitchfork bifurcation of the system (1) has been carefully and rigorously studied, with the aim of contributing to the understanding of the dynamics of the system.

By preforming numerical simulations, for $(r,m,g,k_3)=(3,1,2,1)$, equation (11) becomes

$$F(x_1,\varepsilon)=-\frac{3}{8}\left(\varepsilon+\frac{9}{32}\varepsilon^2\right)x_1-\frac{3}{2}x_1^3.$$

As shown in Fig. 5, the system (1) undergoes a pitchfork bifurcation, which accords with Theorem 2.

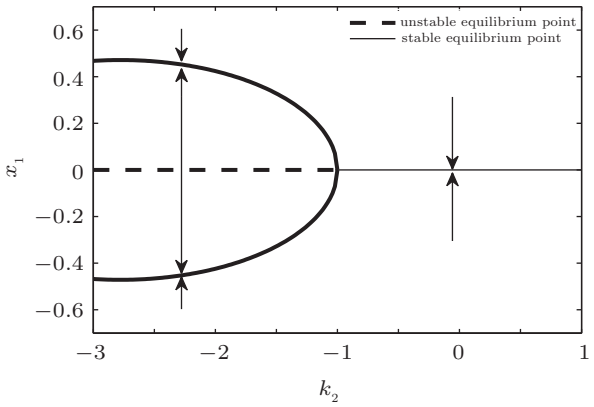


Fig. 5. The pitchfork bifurcation diagram in the system (1) near $k_2=-1$.

5. Ultimate bound estimation of system (1)

Now we utilize the unified approach[16] to derive the ultimate bound of the system (1).

Theorem 3 For $r>0$, $m>0$, $k_3\geq 0$, $k_1,k_2\in R$, and $p_{ii}>0$, $i=1,2,3,4$ satisfying

$$\begin{aligned} &p_{22}=(m+1)gp_{33}+p_{44}, \ \ ((m+1)p_{11}p_{44}-m^2gp_{22}p_{33})g>0, \ \ (m+k_2)mp_{22}-rp_{11}<0, \\ &((m+k_2)mp_{22}-rp_{11})\left(8(m+1)p_{22}p_{44}-(p_{22}-mgrp_{33}+(m+2)p_{44})^2\right) \\ &\quad +(m+1)^2p_{22}((r+1)gmp_{33}-(m+k_2)p_{44})^2<0, \end{aligned} \tag{12}$$

the following set

$$\Omega=\left\{X\left|\begin{array}{c}\left(p_{11}-\dfrac{m^2gp_{22}p_{33}}{(m+1)p_{44}}\right)x^2+p_{33}\left(z+\dfrac{rp_{11}+mp_{22}+k_2p_{44}}{(m+1)gp_{33}}\right)^2 \\ +p_{22}\left(y-\dfrac{p_{44}}{p_{22}}w\right)^2+\dfrac{m^2gp_{22}p_{33}}{(m+1)p_{44}}\left(x-\dfrac{(m+1)p_{44}}{mp_{22}}w\right)^2\leq R_{\max}\end{array}\right.\right\}$$

is the ultimate bound region for the system (1), where $X=(x,y,z,w)^{\mathrm{T}}\in R^4$ and $R_{\max}$ is a real number determined by computing the following maximum optimization question:

$$\begin{aligned} \max \quad V(X)=&\left(p_{11}-\frac{m^2gp_{22}p_{33}}{(m+1)p_{44}}\right)x^2+p_{33}\left(z+\frac{rp_{11}+mp_{22}+k_2p_{44}}{(m+1)gp_{33}}\right)^2 \\ &+p_{22}\left(y-\frac{p_{44}}{p_{22}}w\right)^2+\frac{m^2gp_{22}p_{33}}{(m+1)p_{44}}\left(x-\frac{(m+1)p_{44}}{mp_{22}}w\right)^2, \end{aligned}$$

s.t.

$$\begin{aligned} &\frac{(m+k_2)mp_{22}-rp_{11}}{m+1}x^2-(m+1)p_{22}y^2-k_3p_{33}z^2-2p_{44}w^2+((1+r)mgp_{33}-(m+k_2)p_{44})xw \\ &+(p_{22}-mgrp_{33}+(m+2)p_{44})yw+\left((g-k_1)p_{33}-\frac{k_3(rp_{11}+mp_{22}+k_2p_{44})}{(m+1)g}\right)z \end{aligned}$$

$$+\frac{(rp_{11}+mp_{22}+k_2p_{44})(g-k_1)}{(m+1)g}=0.$$

Proof Rewrite the system (1) into the HDQADS vector form[16,17]

$$\dot{X}=AX+xB_1X+yB_2X+zB_3X+wB_4X+C,$$

where

$$A=\begin{pmatrix}-r & r & 0 & 0\\ m & -1-m & 0 & 1\\ 0 & 0 & -k_3 & 0\\ -k_2 & 0 & 0 & -1\end{pmatrix},$$

$$B_1=\begin{pmatrix}0 & 0 & 0 & 0\\ 0 & 0 & 1/2 & 0\\ mg & -(m+1)g/2 & 0 & 0\\ 0 & 0 & 1/2 & 0\end{pmatrix},$$

$$B_2=\begin{pmatrix}0 & 0 & 0 & 0\\ 0 & 0 & 0 & 0\\ -(m+1)g/2 & 0 & 0 & 0\\ 0 & 0 & 0 & 0\end{pmatrix},$$

$$B_3=\begin{pmatrix}0 & 0 & 0 & 0\\ 1/2 & 0 & 0 & 0\\ 0 & 0 & 0 & 0\\ 1/2 & 0 & 0 & 0\end{pmatrix},$$

$$B_4=\begin{pmatrix}0 & 0 & 0 & 0\\ 0 & 0 & 0 & 0\\ 0 & 0 & 0 & 0\\ 0 & 0 & 0 & 0\end{pmatrix},$$

$$C=\begin{pmatrix}0\\ 0\\ g-k_1\\ 0\end{pmatrix},\quad X=\begin{pmatrix}x\\ y\\ z\\ w\end{pmatrix},$$

and all elements of B_1, B_2, B_3, and B_4 satisfy

$$b_{ij}^k=b_{ik}^j,\ \ (i,j,k=1,2,3,4).$$

Let

$$P=(p_{ij})_{4\times4}\in R^{4\times4},$$
$$p_{ij}=p_{ji}\ \ (i,j=1,2,3,4),$$
$$u=(u_1,u_2,u_3,u_4).$$

We can obtain

$$\begin{aligned}&xX^{\mathrm{T}}(B_1{}^{\mathrm{T}}P+PB_1{}^{\mathrm{T}})X+yX^{\mathrm{T}}(B_2{}^{\mathrm{T}}P+PB_2{}^{\mathrm{T}})X+zX^{\mathrm{T}}(B_3{}^{\mathrm{T}}P+PB_3{}^{\mathrm{T}})X+wX^{\mathrm{T}}(B_4{}^{\mathrm{T}}P+PB_4{}^{\mathrm{T}})X\\ &=2mgp_{13}x^3+2mgp_{34}x^2w-2(m+1)gp_{23}xy^2+2(p_{23}+p_{34})xz^2+2g(mp_{23}-(m+1)p_{13})x^2y\\ &\quad+2(p_{12}+p_{14}+mgp_{33})x^2z2(p_{22}+p_{24}-(m+1)gp_{33})xyz-2(m+1)gp_{34}xyw+2(p_{24}+p_{44})xzw.\end{aligned}$$

By Theorem 1 in Ref. [16], we have

$$xX^{\mathrm{T}}(B_1{}^{\mathrm{T}}P+PB_1{}^{\mathrm{T}})X+yX^{\mathrm{T}}(B_2{}^{\mathrm{T}}P+PB_2{}^{\mathrm{T}})X+zX^{\mathrm{T}}(B_3{}^{\mathrm{T}}P+PB_3{}^{\mathrm{T}})X+wX^{\mathrm{T}}(B_4{}^{\mathrm{T}}P+PB_4{}^{\mathrm{T}})X=0$$

for any $X=(x,y,z,w)^{\mathrm{T}}\in R^4$. So let

$$\begin{aligned}&p_{12}=p_{21}=p_{13}=p_{31}=p_{23}=p_{32}=p_{34}=p_{43}=0,\\ &p_{14}=p_{41}=-mgp_{33},\ \ p_{24}=p_{42}=-p_{44},\\ &p_{22}=(m+1)gp_{33}+p_{44}.\end{aligned}$$

Thus, we obtain

$$P=\begin{pmatrix}p_{11} & 0 & 0 & -mgp_{33}\\ 0 & p_{22} & 0 & -p_{44}\\ 0 & 0 & p_{33} & 0\\ -mgp_{33} & -p_{44} & 0 & p_{44}\end{pmatrix},$$

$$M=uA+2C^{\mathrm{T}}P=(mu_2-ru_1-k_2u_4,\ ru_1-(m+1)u_2,\ 2(g-k_1)p_{33}-k_3u_3,\ u_2-u_4),$$

$$Q=A^{\mathrm{T}}P+PA+(\ B_1{}^{\mathrm{T}}u^{\mathrm{T}}\ \ B_2{}^{\mathrm{T}}u^{\mathrm{T}}\ \ B_3{}^{\mathrm{T}}u^{\mathrm{T}}\ \ B_4{}^{\mathrm{T}}u^{\mathrm{T}}\ )^{\mathrm{T}}$$

$$=\begin{pmatrix}q_{11} & q_{12} & q_{13} & (1+r)mgp_{33}-(m+k_2)p_{44}\\ q_{21} & -2(m+1)p_{22} & 0 & p_{22}-mgrp_{33}+(m+2)p_{44}\\ q_{31} & 0 & -2k_3p_{33} & 0\\ (1+r)mgp_{33}-(m+k_2)p_{44} & p_{22}-mgrp_{33}+(m+2)p_{44} & 0 & -4p_{44}\end{pmatrix},$$

where

$$q_{11}=-2rp_{11}+2mgk_2p_{33}+mgu_3,\ \ q_{12}=q_{21}=rp_{11}+mp_{22}+k_2p_{44}-\frac{(m+1)g}{2}u_3,$$

$$q_{13} = q_{31} = \frac{u_2 + u_4}{2}.$$

For simplifying Q, we take

$$u = \left(0, 0, \frac{2(rp_{11} + mp_{22} + k_2 p_{44})}{(m+1)g}, 0\right).$$

Now we have

$$M = \left(0,\ 0,\ 2(g-k_1)p_{33} - \frac{2k_3(rp_{11} + mp_{22} + k_2 p_{44})}{(m+1)g},\ 0\right),$$

$$Q = \begin{pmatrix} \frac{2((m+k_2)mp_{22} - rp_{11})}{m+1} & 0 & 0 & (1+r)mgp_{33} - (m+k_2)p_{44} \\ 0 & -2(m+1)p_{22} & 0 & p_{22} - mgrp_{33} + (m+2)p_{44} \\ 0 & 0 & -2k_3 p_{33} & 0 \\ (1+r)mgp_{33} - (m+k_2)p_{44} & p_{22} - mgrp_{33} + (m+2)p_{44} & 0 & -4p_{44} \end{pmatrix}.$$

We obtain the Lyapunov-like quadratic function

$$\begin{aligned} V(X) &= X^{\mathrm{T}}PX + uX + \frac{1}{4}uP^{-1}u^{\mathrm{T}} \\ &= \left(p_{11} - \frac{m^2 g p_{22} p_{33}}{(m+1)p_{44}}\right)x^2 + p_{33}\left(z + \frac{rp_{11} + mp_{22} + k_2 p_{44}}{(m+1)gp_{33}}\right)^2 + p_{22}\left(y - \frac{p_{44}}{p_{22}}w\right)^2 + \frac{m^2 g p_{33} p_{22}}{(m+1)p_{44}}\left(x - \frac{(m+1)p_{44}}{mp_{22}}w\right)^2, \end{aligned}$$

and the derivative along with the system (1)

$$\begin{aligned} \dot{V}(X) &= X^{\mathrm{T}}QX + MX + uC \\ &= \frac{2((m+k_2)mp_{22} - rp_{11})}{m+1}x^2 - 2(m+1)p_{22}y^2 - 2k_3 p_{33}z^2 - 4p_{44}w^2 \\ &\quad + 2\left((1+r)mgp_{33} - (m+k_2)p_{44}\right)xw + 2\left(p_{22} - mgrp_{33} + (m+2)p_{44}\right)yw \\ &\quad + 2\left((g-k_1)p_{33} - \frac{k_3(rp_{11} + mp_{22} + k_2 p_{44})}{(m+1)g}\right)z + \frac{2(rp_{11} + mp_{22} + k_2 p_{44})(g-k_1)}{(m+1)g} = 0. \end{aligned}$$

By $r > 0$, $m > 0$, $k_3 \geq 0$, $p_{ii} > 0$ $(i = 1,2,3,4)$ and Eq. (12), we obtain $P > 0$ and $Q < 0$. Hence Theorem 3 is proved.

By numerical simulations, for $(m, r, g, k_1, k_2, k_3, p_{11}, p_{33}, p_{44}) = (1, 6, 0.12, 0.12, 1, 0.001, 1.1, 0.5, 4)$, we have $P > 0$ and $Q < 0$. By using Lingo to solve the corresponding optimization problem, we obtain $R_{\max} = 2640.2$ for $(x, y, z, w) = (0, 0, 0, 0)$. Therefore, the corresponding ultimate bound region of the hyperchaotic attractor is given by

$$\Omega = \left\{ X \in R^4 \middle| \, 1.07x^2 + 0.5(z + 72.67)^2 + 0.06(0.75x - 1.34w)^2 + (1.06y - 0.94w)^2 \leq 2640.2 \right\}.$$

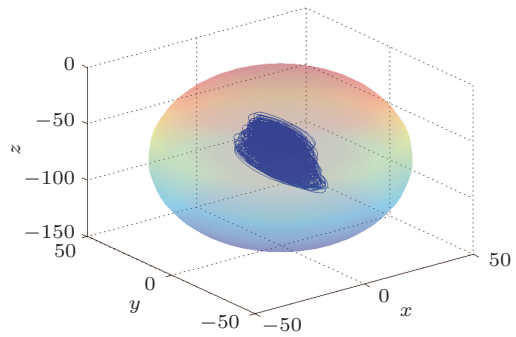


Fig. 6. (color online) The hyperchaotic attractor of the system (1) with $(m, r, g, k_1, k_2, k_3) = (1, 6, 0.12, 0.12, 1, 0.001)$ and its ultimate bound estimated with $(p_{11}, p_{33}, p_{44}) = (1.1, 0.5, 4)$ in the (x, y, z) space and $w = 0$.

Table 1 shows numerically actual and estimated bounds of the hyperchaotic attractor. In order to illustrate the bound vividly, figure 6 shows the phase portraits of the hyperchaotic attractor.

Table 1. The estimated bound of the hyperchaotic attractor.

Variable	Actual bound	Estimated bound set Ω
x	$(-9.7007, 8.7668)$	$(-48.9084, 48.9084)$
y	$(-30.3310, 28.9109)$	$(-48.4744, 48.4744)$
z	$(-84.5560, -49.274)$	$(-145.3364, -0.0036)$
w	$(-33.8435, 33.2820)$	$(-51.6069, 51.6069)$

6. Conclusions

The 4D segmented disc dynamo is very interesting and reported rarely, in that it possesses coexisting hidden attractors with only one stable equilibrium or a line equilibrium. In addition, by choosing an appropriate bifurcation parameter, the paper proves that the Hopf bifurcation and pitchfork bifurcation occur in the system. Also, the ellipsoidal ultimate bound is obtained. Numerical simulations are done to demonstrate the emergence of the two bifurcations and show the ultimate

boundary region.

It is hoped that the investigation of this paper can be quite beneficial to further studies of the dynamically rich segmented disc dynamo, which is very desirable for magnetic field generation and reversals in astrophysical bodies, and will shed some light leading to final revealing the true geometrical structure of the attractor of the amazing original system.

Acknowledgments

We express our sincere thanks to the anonymous referees for their rigorous comments and valuable suggestions helping to improve the original manuscript.

References

[1] Wang Z, Ding S, Shan Q and Zhang H 2016 *IEEE Trans. Neural Netw. Learn. Syst.*
[2] Ding S, Wang Z and Zhang H 2016 *International Journal of Control*
[3] Chang C Y, Zhao X, Yang F and Wu C E 2016 *Chin. Phys. B* **25** 070504
[4] Lei Y M and Zhang H X 2017 *Chin. Phys. B* **26** 030502
[5] Ojoniyi O S and Njah A N 2016 *Chaos, Solitons and Fractals* **87** 172
[6] Wei Z, Wang R and Liu A 2014 *Math. Comput. Simul.* **100** 13
[7] Wei Z and Zhang W 2014 *Int. J. Bifur. Chaos* **24** 1450127
[8] Wang X and Chen G 2012 *Commun. Nonlinear Sci. Numer. Simul.* **17** 1264
[9] Molaie M, Jafari S and Sprott J C 2013 *Int. J. Bifur. Chaos* **23** 1350188
[10] Jafari S and Sprott J C 2013 *Chaos, Solitons and Fractals* **57** 79
[11] Liu Y and Yang Q 2010 *Nonlinear Anal. RWA* **11** 2563
[12] Moffatt H K 1979 *Geophys. Astrophys. Fluid Dyn.* **14** 147
[13] Sprott J C 2011 *Int. J. Bifur. Chaos* **21** 2391
[14] Kuznetsov Y A 1998 Elements of Applied Bifurcation Theory (New York: Springer-Verlag)
[15] Wiggins S 1990 *Introduction to Applied Nonlinear Dynamical Systems and Chaos* (New York: Springer-Verlag)
[16] Wang P, Li D, Wu X, Lv J and Yu X 2011 *Int. J. Bifur. Chaos* **21** 2679
[17] Wang J, Zhang Q, Chen Z and Li H 2014 *Nonlinear Dyn.* **78** 2517